

## POTASSIUM CARBONATE-TREATED PALM KERNEL SHELL ADSORBENT FOR CONGO RED REMOVAL FROM WATER

Lee Lin Zhi, Muhammad Abbas Ahmad Zaini\*

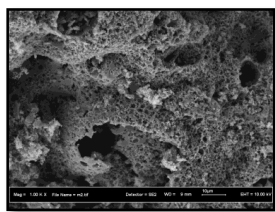
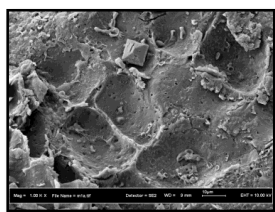
Centre of Lipids Engineering & Applied Research (CLEAR), Ibnu  
Sina ISIR, Universiti Teknologi Malaysia, 81310 utm Johor Bahru,  
Johor, Malaysia

### Article history

Received  
7 January 2015  
Received in revised form  
15 February 2015  
Accepted  
15 June 2015

\*Corresponding author  
abbas@cheme.utm.my

### Graphical abstract



### Abstract

This work was aimed to evaluate the adsorptive characteristics of potassium carbonate-treated palm kernel shell adsorbent for the removal of congo red from water. The adsorbent was characterized according to the specific surface area, surface morphology and surface functional groups. The bottle-point technique was employed to investigate the equilibrium uptake and the adsorption kinetics of congo red, and the removal mechanisms were proposed from the widely used isotherm and kinetics models. Results show that the specific surface area of adsorbent increased after the treatment rendering the maximum congo red uptake of 8.0 mg/g. The removal of congo red obeyed Langmuir isotherm and pseudo-second-order kinetics model suggesting the chemically-attributed homogeneous adsorption. Regeneration of congo red-loaded adsorbent by irradiated water showed a better regeneration efficiency of 82%. Palm kernel shell is a promising adsorbent candidate for congo red removal from water.

**Keywords:** Adsorption, congo red, adsorbent, palm kernel shell, chemical treatment, regeneration

### Abstrak

Over Kajian ini bertujuan menilai ciri-ciri penjerapan bahan penjerap isirong sawit terawat kalium karbonat untuk penyingkiran kongo merah daripada air. Penjerap dicirikan berdasarkan luas permukaan spesifik, morfologi permukaan dan kumpulan berfungsi permukaan. Teknik titik-botol digunakan untuk mengkaji pengambilan keseimbangan dan kinetik penjerapan kongo merah, dan mekanisma penyingkiran dicadangkan daripada model-model isoterma dan kinetik yang meluas digunakan. Hasil kajian menunjukkan bahawa luas permukaan spesifik penjerap meningkat selepas rawatan memberikan pengambilan maksimum kongo merah sebanyak 8.0 mg/g. Penyingkiran kongo merah mematuhi isoterma Langmuir dan model kinetik pseudo-tertib kedua yang mencadangkan penjerapan homogen bersifat kimia. Penjanaan semula penjerap termuat kongo merah dengan air teriradiasi menunjukkan kecekapan penjanaan semula lebih baik dengan 82%. Isirong sawit adalah calon penjerap yang sesuai untuk penyingkiran kongo merah daripada air.

**Kata kunci:** Isirong sawit, kongo merah, penjanaan semula, penjerap, penjerapan, rawatan kimia

© 2015 Penerbit UTM Press. All rights reserved

## 1.0 INTRODUCTION

There is an increasing concern over the environmental problems due to rapid generation of

wastes and improper management of industrial effluents. The pollutants from textile industry are declared as one of the major sources of wastewater in ASEAN countries.

Congo red is a benzenedene dye. It is mainly used in textile, paper, printing, leather industry, and in the wastewater discharges. It can cause allergic reactions and irritate the skin, eyes and gastrointestinal tract. In addition, the decomposition products of congo red such as carbon monoxide, oxide of nitrogen and oxide of sulfur are carcinogen [1]. Due to its complex chemical structure, congo red is difficult to be degraded. Besides, it has high solubility an aqueous solution and persistence in the natural environment [2].

Adsorption is among the most suitable technique to remove dye from water due to its process convenient, easy to operate, simple design and wide range of available adsorbents. It is also inexpensive and does not produce sludge [1]. Activated carbon is a widely used adsorbent due to its large porous surface area, controlled pore structure and inert properties. However, commercially available activated carbon is cost prohibitive. In addition, the regeneration of spent activated carbon usually leads to 10-15% loss of the adsorbent yield and also the absorption capacity [3]. Therefore, finding an abundantly available and low cost adsorbent precursor has become a subject of considerable interest.

One of the promising candidate under this category is palm kernel shell. It can be activated into high porosity carbon in short time due to its high lignin content, low cellulose content and less fibrous structure (Table 1). It is considered abundance and renewable source in palm oil producing countries like Indonesia and Malaysia. The use of palm kernel shell as adsorbent precursor is expected to greatly reduce the inherent costs. Moreover, the issues revolving around the management of oil palm waste can also be reduced [4].

**Table 1** Composition of some oil palm wastes [5, 6]

Oil palm waste	Lignin (wt%)	Cellulose (wt%)
Palm kernel shell	44.5	26.7
Palm empty fruit bunch	13.0-37.0	43.0-65.0
Palm frond	20.0-21.0	40.0-50.0
Palm trunk	18.0-23.0	29.0-37.0

Adsorbent can be prepared through chemical treatment. It involves impregnating the adsorbent with dehydrating agent such as  $K_2CO_3$ ,  $ZnCl$  or  $KOH$ . Chemical treatment offers some advantages over physical treatment; single-step process, low activation temperature, and shorter processing time, higher yield and better performance [7]. Potassium carbonate is preferably used in adsorbent preparation because of its non-hazardous properties and non-deleterious compared to  $KOH$  and  $NaOH$  [8].

This work was aimed to evaluate the adsorptive characteristics of potassium carbonate-treated palm kernel shell adsorbent for congo red dye removal

from water. The adsorbent was characterized and the adsorption data were analyzed using the widely used isotherm and kinetics models. The removal mechanisms were also discussed. Lastly, the regeneration of spent adsorbent was studied.

## 2.0 EXPERIMENTAL

### 2.1 Preparation of Adsorbent

Palm kernel shell was obtained from Felda Taib Andak, Kulai, Johor. Congo red, C.I. No. 22120, MW = 696.65 g/mol and  $\lambda_{max} = 487 - 500nm$  was purchased from R&M Marketing, Essex. Potassium carbonate anhydrous powder,  $K_2CO_3$  (99.5%) and hydrochloride acid,  $HCl$  (37.0%) were used without further purification. All chemicals are analytical-grade reagents.

The adsorbent was prepared by mixing the desired weight of palm kernel shell with  $K_2CO_3$  solution at impregnation ratio of 1.0. The mixture was homogeneously stirred on hot plate at  $90^\circ C$  for 1.5h. The mixture was then dried in oven at  $110^\circ C$  for 24h. The impregnated precursor was heated in furnace at  $550^\circ C$  for 1.5h, and the resultant product was soaked in 3M  $HCl$  overnight for partial demineralization and to remove excess  $K_2CO_3$ . Thereafter, the adsorbent was washed with distilled water to a constant pH. The adsorbent was dried in oven at  $110^\circ C$ , and stored prior to use.

### 2.2 Characterization of Adsorbent

Potassium carbonate-treated adsorbent was characterized according to the specific surface area, morphology and surface functional groups. The specific surface area was determined by Pulse Chemi Sorb 2705 with liquid  $N_2$  at 77K. Surface morphology was observed using Field Emission Scanning Electron Microscope at 1000 times magnification (SUPRA 35VP). Fourier Transform Infrared Spectroscopy instrument (Spectrum One) with  $KBr$  pellet was used to obtain the peaks of functional groups at  $400-4000\text{ cm}^{-1}$ .

### 2.3 Removal of Congo Red

About 0.05g adsorbent was brought into intimate contact with 50mL of congo red solution at varying concentrations. The mixtures were allowed to equilibrate at  $25^\circ C$  and 120rpm for 72h. The removal of congo red was calculated as,

$$q_e = \frac{(C_0 - C_e)}{m} V \quad (1)$$

where  $q_e$  is the equilibrium removal (mg/g),  $C_0$  is the initial congo red concentration (mg/L),  $C_e$  is the equilibrium congo red concentration (mg/L),  $m$  is mass of adsorbent (g) and  $V$  is volume of solution (L). The congo red concentration was measured using

visible spectrophotometer (Biochrom Libra S6) at wavelength of 500nm. The calibration curve is linear through origin; a.u. = 0.0549 × concentration (mg/L) with  $R^2 = 0.992$ . The adsorption data were analyzed using isotherm models, namely Langmuir and Freundlich models. The Langmuir model describes monolayer adsorption on the homogenous surface and is expressed as,

$$q_e = \frac{QbC_e}{1 + bC_e} \quad (2)$$

where  $Q$  is the monolayer adsorption capacity (mg/g), and  $b$  is the Langmuir constant (L/g). The Freundlich equation describes the adsorption onto heterogeneous adsorbent surface and is given as,

$$q_e = KC_e^{1/n} \quad (3)$$

where  $K$  and  $n$  are the Freundlich constants. The Redlich-Peterson model that combines both features of Langmuir and Freundlich models is given as,

$$q_e = \frac{AC_e}{1 + BC_e^g} \quad (4)$$

where  $A$ ,  $B$  and  $g$  are all the Redlich-Peterson constant, and  $0 < g < 1$ .

Kinetics study was performed at two initial concentrations of congo red, i.e., 20 and 50mg/L. About 0.05g of adsorbent was added into a series of flasks containing 50mL of congo red solution, and the residual concentration was measured at varying time intervals. The effect of time on congo red removal was determined as,

$$q_t = \frac{(C_0 - C_t)}{m} V \quad (5)$$

where  $q_t$  the amount of dye adsorbed at time  $t$  (mg/g) and  $C_t$  is the concentration of congo red at time  $t$  (mg/L). Kinetic models were applied to investigate the removal mechanisms of congo red onto adsorbent. Pseudo-first-order equation indicates diffusion-type sorption and is expressed as,

$$q_t = q_e(1 - e^{-k_1 t}) \quad (6)$$

where  $q_e$  is the calculated equilibrium adsorption (mg/g) and  $k_1$  is the rate constant of the pseudo-first-order adsorption. Pseudo-second order equation indicates the chemical-type adsorption is given as,

$$q_t = \frac{k_2 q_e^2 t}{1 + k_2 q_e t} \quad (7)$$

where  $k_2$  is the rate constant of the pseudo-second-order adsorption. All isotherm and kinetics constants were determine by non-linear regression using Solver add-in of Microsoft Excel for the least sum of squared error (SSE) and optimum coefficient of determination ( $R^2$ ).

## 2.4 Regeneration of Spent Adsorbent

Three cycles of adsorption were performed using the regenerated adsorbent. Regeneration of congo red loaded adsorbent was carried out using sodium hydroxide and irradiated water. The spent adsorbent was immersed in 50 mL of 0.1M NaOH at ambient temperature for 3 h. Then the adsorbent was rinsed twice with hot water. For microwave-assisted regeneration (also termed irradiated water), the spent adsorbent was added in Teflon mould containing 50 mL of distilled water. It was then heated in microwave at power intensity of 70% for 5min. The desorption of congo red was calculated as,

$$q_d = \frac{C_d - C_0}{m} V \quad (8)$$

where  $q_d$  is the equilibrium dye concentration on the adsorbent (mg/g),  $C_0$  is the initial concentration of congo red in solution ( $C_0 = 0$ ) and  $C_d$  is equilibrium concentration after desorption (mg/L). Recovery of adsorbent was calculated as,

$$recovery = \frac{m_{e_n}}{m_0} \times 100\% \quad (9)$$

where  $m_{e_n}$  is mass of adsorbent after  $n^{\text{th}}$  cycle of regeneration (g) and  $m_0$  is the initial mass before the first commence of regeneration (g). The regeneration efficiency was determined as,

$$efficiency = \frac{q_{e_n}}{q_{e_0}} \times 100\% \quad (10)$$

where  $q_{e_0}$  is the adsorption capacity of fresh adsorbent (mg/g) and  $q_{e_n}$  is the adsorption capacity of the regenerated adsorbent after  $n^{\text{th}}$  regeneration cycle (mg/g).

## 3.0 RESULTS AND DISCUSSION

### 3.1 Characteristics of Adsorbent

The raw palm kernel shell contains 12% moisture and 1.3% ash. Upon  $K_2CO_3$  treatment, the yield of adsorbent is 20.1%. The lower yield is likely due to the gasification of palm shell char by  $K_2CO_3$ . The presence of  $K_2CO_3$  in the interior of the precursor restricts the formation of tar by the formation of cross-links, and inhibits the shrinkage of precursor particle by occupying certain substantial volume [9]. However, the char tends to react with  $K_2CO_3$  in inert atmosphere and be liberated in the gasification.

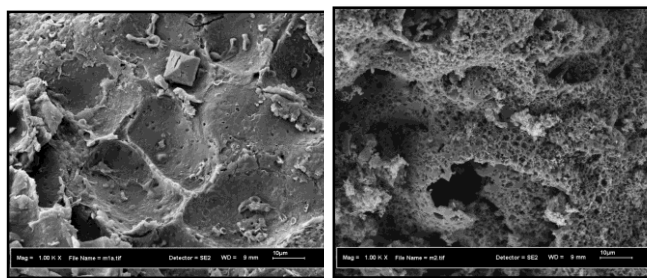


Figure 1 FESEM images of (a) palm kernel shell and (b)  $K_2CO_3$ -treated palm kernel shell adsorbent

Figure 1(a) shows the surface of raw palm kernel shell was observed to be rough and dented, where pores are not observed on the surface, while the chemically-treated adsorbent displays well-developed micro-textures that could be resulted from the reaction between  $K_2CO_3$  and carbon. The heat treatment of char at  $550^\circ C$  is likely to enhance the specific surface area and pore volume of the adsorbent by promoting the diffusion of  $K_2CO_3$  into the pores and thereby increasing the  $K_2CO_3$ -carbon reaction [10]. According to Hayashi and co-workers [11], the total pore volume of adsorbent could be increased when higher treatment temperature was employed. However, the treatment at temperature higher than  $550^\circ C$  decreases the yield, and the uncompleted reaction might cause the surface pores to be blocked by  $K_2CO_3$ .

The specific surface areas for palm kernel shell and its derived adsorbent were recorded as 2.8 and  $54 m^2/g$ , respectively. The values are in agreement with the surface morphology (Figure 1). The presence of  $K_2CO_3$  at  $550^\circ C$  has resulted in the increasing of carbon "burn-off". The devolatilization of char develops the rudimentary pore structure, whereas the  $K_2CO_3$ -carbon reaction enhances the existing pores and created new porosities so as to increase the specific surface area and pore volume [11]. This subsequently decreased the adsorbent yield. According to Adinata *et al.* [8], the specific surface area is decreased due to the enlargement of micropores to mesopores when higher concentration of  $K_2CO_3$  is used in the adsorbent preparation.

Table 2 summarizes the peaks and respective surface functional groups in palm kernel shell and its chemically-treated adsorbent. Palm kernel shell exhibits different peaks of varying intensities indicating the presence of surface functional groups. The functional groups are hydroxyl group O-H, methylene C-H, aldehyde, C=O, aromatic C=C and primary alcohol C-O. However, considerable fractions of the absorption peaks of the derived adsorbent were diminished. It is suggested that the functional groups are evaporated as volatile materials due to the treatment with  $K_2CO_3$  [12].

Table 2 Absorption frequency and FTIR assignment for palm kernel shell and its adsorbent derivative

Functional Group	Absorption frequency found in samples ( $cm^{-1}$ )	
	Palm kernel shell	Adsorbent
O-H stretch	3400	3467
Methylene C-H asym./sym. stretch	2923	-
Aldehyde, C=O stretch	1737	-
C=C aromatic ring stretch	1608, 1459	-
Primary alcohol, C-O stretch	1048	-

### 3.2 Removal of Congo Red

#### 3.2.1 Equilibrium Isotherm

The pH of the congo red solution was not adjusted, and the average value was recorded as  $4.9 \pm 0.92$  upon equilibrium. Figure 2 shows the equilibrium removal of congo red by palm kernel shell based adsorbent. The adsorbent clearly demonstrates an increasing trend in the adsorption capacity as the equilibrium concentration increases until a saturation point of  $8 mg$  congo red per gram of adsorbent is reached at  $C_e = 12 mg/L$ . At lower concentration, the ratio of initial number of dye molecules to the available surface area is low, thus, the fractional adsorption becomes independent on the initial concentration. However, at higher concentration, the available sites of adsorption become fewer, subsequently, no active site available for further binding of dye molecules to surface of adsorbent, at which equilibrium adsorption is achieved. Attempt was also made to remove congo red by untreated palm kernel shell, yet no significant change in concentration was observed. The results are supported by the surface morphology and specific surface area of the chemically-treated adsorbent.

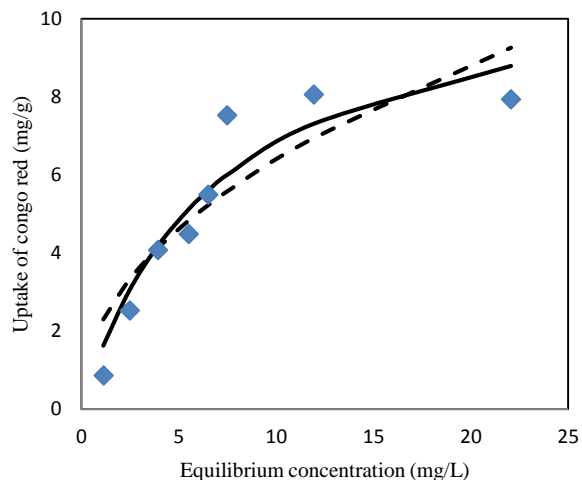


Figure 2 Equilibrium removal of congo red by potassium carbonate-treated adsorbent. Lines were predicted by Langmuir and Redlich-Peterson (solid), and Freundlich (dashed) models

**Table 3** Constants of isotherm models

Langmuir model	
Q (mg/g)	11.6
b (L/mg)	0.144
SSE	4.9
R <sup>2</sup>	0.91
Freundlich model	
K	2.17
1/n	0.469
SSE	9.7
R <sup>2</sup>	0.81
Redlich-Peterson model	
A (L/g)	1.67
B	0.144
g	1
SSE	4.9
R <sup>2</sup>	0.91

The equilibrium data were analyzed using the three isotherm models, namely Langmuir, Freundlich and Redlich-Peterson models. Table 3 summarizes the constants of isotherm models for the removal of congo red by palm kernel shell based adsorbent. It was found that the adsorption of congo red onto the adsorbent can be described by Langmuir model due to R<sup>2</sup> is closer to 1. The applicability of Langmuir model indicates that the adsorption process is favorable and it corresponds to the homogeneous nature of the surfaces of adsorbent and the formation of monolayer coverage of dye molecule at the outer surface of adsorbent. The g value of Redlich-Peterson that equals to one also suggests that the adsorption is monolayer in nature.

### 3.2.2 Adsorption Kinetics

The effect of contact time was investigated to determine the rate constants and time required to attain the equilibrium. Two initial dye concentrations were evaluated, i.e., 5 and 15 mg/L. Figure 3 displays the adsorption kinetics of congo red by palm kernel shell based adsorbent. The adsorption of congo red was rapid at the beginning, and for both concentrations studied the equilibrium was attained at time = 48 h, where no remarkable change in concentration was observed thereafter. Two kinetic models, i.e., pseudo-first order and pseudo-second order models were used to explicate the adsorption mechanism of congo red onto the adsorbent.

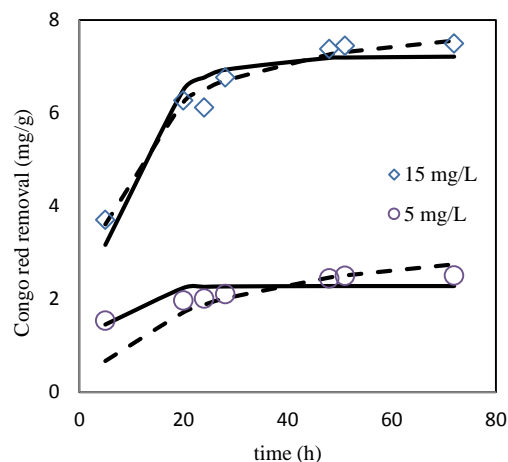


**Figure 3** Kinetics of congo red removal by potassium carbonate-treated adsorbent. Lines were predicted by pseudo-first-order (solid) and pseudo-second-order (dashed) models

**Table 4** Constants of kinetics models

C <sub>0</sub> (mg/L)	5	15
q <sub>e, meas</sub> (mg/g)	2.5	7.5
Pseudo-first-order		
q <sub>e, cal</sub> (mg/g)	2.3	7.2
k <sub>1</sub> (h <sup>-1</sup> )	0.203	0.116
SSE	0.293	0.961
R <sup>2</sup>	0.716	0.928
Pseudo-second-order		
q <sub>e, cal</sub> (mg/g)	2.4	8.2
k <sub>2</sub> (g/mg.h)	0.028	0.019
SSE	0.908	0.192
R <sup>2</sup>	0.958	0.982

q<sub>e, meas</sub>: measured equilibrium uptake; q<sub>e, cal</sub>: calculated equilibrium uptake

The constants of kinetics models are tabulated in Table 4. From Figure 3 and Table 4, it can be found that the fitting of experimental data to the pseudo-first-order model is not as good as to the pseudo-second-order model. It indicates that the experimental data well obeyed the pseudo-second-order model. Pseudo-second-order reaction is mainly dependent on the amount of dye adsorbed on the surface of adsorbent and the amount adsorbed at equilibrium, where the dye molecules stick to the adsorbent surface forming a chemical bond [13]. Similar results were reported for adsorption kinetic of congo red onto coir pith based activated carbon [14] and commercial activated carbon [15]. It is also useful to note that the pseudo-second-order rate constant, k<sub>2</sub> for lower concentration (5 mg/L) is greater than that at higher concentration (15 mg/L). It could be due to lower activation energy at lower concentration [13]. Furthermore, the dye molecules could be bonded to the active sites on the adsorbent surface at much faster rate when the concentration is low due to the less interactions.

### 3.3 Regeneration of Spent Adsorbent

Recovery is an important economic factor of regeneration process. Chemically-regenerated adsorbent has lower recovery compared to one through microwave-assisted regeneration. It is likely due to loss of adsorbent during the extensive washing process. The values were recorded as 91 and 98wt%, respectively.

Figure 4 displays the desorption of congo red and the regeneration efficiency of palm kernel shell based adsorbent. Some of the pre-adsorbed congo red was leached out in the solution during the regeneration of spent adsorbent. Moreover, it was observed that the desorption is preferably occurred in heated water instead of NaOH. Similar finding was reported by Lu and co-workers [16], where alkali solution can be used to desorb dyes with  $-SO_3Na$  and  $-NH_2$  functional groups but the desorption efficiency is less satisfied.

Adsorption performance for both regeneration methods are valid with the results of desorption. More dye molecules are released rendering more surface sites available for subsequent adsorption. It was also found that the regenerated adsorbent exhibits greater adsorption than the amount that previously desorbs. This might be due to the degradation of dye via external environment such as heat and irradiation. Besides, it is likely that the pre-adsorbed dye molecules are not desorbed in regeneration and that there are still vacant sites on the adsorbent to accommodate the dye molecules in the next adsorption cycle.

From Figure 4, the efficiency was found to decrease with increasing the regeneration cycles. This is in agreement with the partial desorption of congo red molecules and the blockage of the porous structure [17]. However, the irradiated water method demonstrates a better regeneration efficiency of adsorbent for three consecutive cycles.

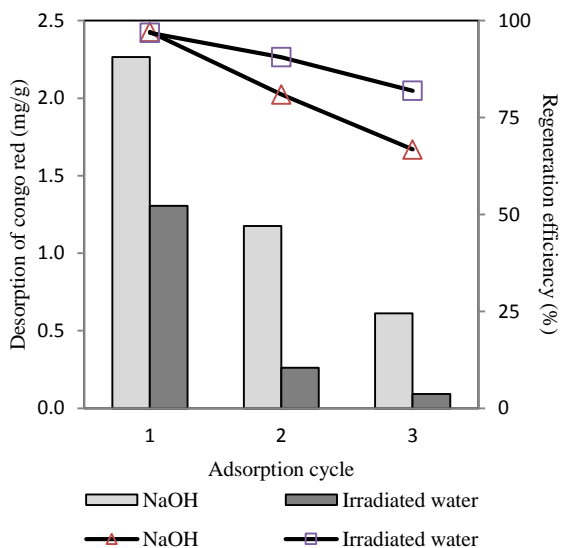


**Figure 4** Desorption of congo red and regeneration efficiency of spent adsorbent for three consecutive cycles

### 4.0 CONCLUSION

Potassium carbonate-treated adsorbent was prepared from palm kernel shell for congo red removal. The specific surface area of adsorbent is  $54m^2/g$  and the maximum uptake of congo red is  $8mg/g$ . The adsorption data fitted well to the Langmuir model, while the kinetics data obeyed pseudo-second-order model. The models suggest that the adsorption of congo red onto adsorbent was monolayer in nature and chemically driven by the surface characteristics of the adsorbent. The microwave-assisted method shows a better regeneration efficiency of adsorbent after three adsorption cycles. With suitable treatment strategies, palm kernel shell can be employed as adsorbent for dyes removal from water.

### Acknowledgement

Authors acknowledge the Fundamental Research Grant Scheme (#4F305) awarded by the Ministry of Education Malaysia. L. Lin-Zhi thanks Ministry of Education Malaysia for the financial assistance through MyBrain15 scholarship.

### References

- [1] Huang, C. J., Y. J. Yang, D. X. Yang, and Y. J. Chen. 2009. Frog Classification Using Machine Learning Techniques. *Expert System Application*. 36: 3737-3743.
- [2] Chesmore, E. D. 2004. Automated Bioacoustic Identification of Species. *Anais DA Academia Brasileira de Ciências*. 76(2): 435-440.
- [3] Fletcher, N. H. 2010. Acoustical Background to the Many Varieties of Birdsong. *Acoustic Australia*. 38(2): 59-62.
- [4] Chesmore, E. D. 2001. Application of Time Domain Signal Coding and Artificial Neural Networks to the Passive Acoustical Identification of Animals. *Applied Acoustic*. 62: 1359-1374.
- [5] Reby, D., S. Lek, I. Dimopoulos, J. Joachim, J. Lauga, and S. Aulagnier. 1997. Artificial Neural Networks as a Classification Method in the Behavioural Sciences. *Behavioural Processes*. 40: 35-43.
- [6] Dietrich, C., G. Palm, and F. Schwenker. 2003. Decision Templates for the Classification of Bioacoustic Time Series. *Information Fusion*. 4: 101-109.
- [7] Kathryn, P. 1996. Where Have All the Frogs and Toads Gone. *Bioscience* 40(6): 2-4.
- [8] Beebee, T. J. C., and Griffiths, R. A. 2005. The Amphibian Decline Crisis: A Watershed for Conservation Biology? *Biological Conservation*. 125(3): 271-285.
- [9] Carey, C. 1997. Kathryn Phillips: 1995, Tracking the Vanishing Frogs, Penguin Books. *Climatic Change*. 37(3): 565-567.
- [10] Tan, W. C., Jaafar H., Ramli, D. A., Rosdi, B. A., and Shahrudin, S. 2014. Intelligent Frog Species Identification on Android Operating System. *International Journal of Circuits, Systems and Signal Processing*. 8: 137-148.
- [11] Yuan, C. L. T., and Ramli, D. A. 2013. Frog Sound Identification System for Frog Species Recognition. *Lecture Notes of the Institute for Computer Sciences, Social Informatics and Telecommunications Engineering*. 109: 41-50.

- [12] Ng, C. H., S. V. Muniandy, and Dayou, J. 2011. Acoustic Classification of Australian Anurans Based on Hybrid Spectral-Entropy Approach. *Applied Acoustic*. 72(9): 639-645.
- [13] Dayou, J., C. H. Ng, C. M. Ho, A. H. Ahmad, S. V. Muniandy, and M. N. Dalimin. 2011. Classification and Identification of Frog Sound Based on Entropy Approach. *International Conference on Life Science and Technology (ICLST 2011)*. 7-9 Januari 2011. Mumbai, India.
- [14] Beck, C. 2009. Generalised Information and Entropy Measures In Physics. *Contemporary Physics*. 50(4): 495-510.
- [15] Buddle, C. M., J. Beguin, E. Bolduc, A. Mercado, and T. E. Sackett. 2005. The Importance and Use of Taxon Sampling Curves for Comparative Biodiversity Research with Forest Arthropod Assemblages. *Canadian Entomologist*. 137: 120-127.
- [16] Sueur, J., S. Pavoine, O. Hamerlynck, and S. Duvail. 2008. Rapid Acoustic Survey for Biodiversity Appraisal. *PLoS ONE*. 3(12): 4065.
- [17] Rényi, A. 1959. On the dimension and entropy of probability distributions. *Acta Mathematica Academiae Scientiarum Hungaricae*. 10: 193-215.
- [18] Rényi, A. 1961. On measures of entropy and information. *Proceedings of the 4th Berkeley Symposium on Mathematics of Stats and Probability*. University of California Press, Berkeley 1: 547-561.
- [19] Csisza' r, I. 1995. Generalized cutoff rates and Rényi's information measures. *IEEE Transactions on Information Theory*. 41: 26-34.
- [20] Vinga, S. and J. S. Almeida. 2004. Rényi continuous entropy of DNA sequences. *Journal of Theoretical Biology*. 231: 377-388.
- [21] Baraniuk, R., P. Flandrin, A. Janssen, and O. Michel. 2001. Measuring time-frequency information content using the Rényi entropies. *IEEE Transactions on Information Theory*. 47: 1391-1409.
- [22] Neemuchwala, H., A. Hero, and P. Carson. 2005. Image matching using alpha-entropy measures and entropic graphs. *Signal Processing*. 85: 277-296.
- [23] Song, K. S. 2001. Rényi information, loglikelihood and an intrinsic distribution measure. *Journal of Statistical Planning and Inference*. 93: 51-69.
- [24] Hart, P. E. 1975. Moment distributions in economics: an exposition. *Journal of the Royal Statistical Society Series A*. 138: 423-434.
- [25] Tsallis, C. 1988. Possible Generalization of Boltzmann-Gibbs Statistics. *Journal of Statistical Physics*. 52:479.
- [26] Yulmetyev, R. M., N. A. Emelyanova, and F. M. Gafarov. 2004. Dynamical Shannon entropy and information Tsallis entropy in complex systems. *Journal of Physics A*. 341: 649-676.
- [27] Hadzibeganovic, T. and S. A. Cannasc. 2009. A Tsallis' statistics based neural network model for novel word learning. *Journal of Physics A*. 388: 732-746.
- [28] Rufiner, H. L., M. E. Torres, L. Gamero, and D. H. Milone. 2004. Introducing complexity measures in nonlinear physiological signals: application to robust speech recognition. *Journal of Physics A*. 332: 496-508.
- [29] Burton, T. C. 1993. Family microhylidae. In: Glasby, C. G., Ross G. J. B, Beesley P. L. (editors). *Fauna of Australia*. 2A. Canberra: AGPS.
- [30] Fletcher, N. H. 2005. Acoustics system in biology: from insect to elephants. *Acoustics Australia*. 33(3): 83-88.
- [31] Fletcher, N. H. 1997. Sound in animal world. *Acoustics Australia*. 25(2): 69-74.